Use of Prandtl-Ishlinskii hysteresis operators for Coulomb friction modeling with presliding

Michael Ruderman
University of Agder (UiA), 4604 Kristiansand, Norway
E-mail: michael.ruderman@uia.no

Dmitrii Rachinskii
University of Texas in Dallas (UTD), 800 W Campbell Road Richardson, Texas, USA
E-mail: dmitry.rachinskiy@utdallas.edu

Abstract. Prandtl-Ishlinskii stop-type hysteresis operators allow for modeling elasto-plasticity in the relative stress-strain coordinates including the saturation level of the residual constant-tension flow. This lies in direct equivalence to the force-displacement characteristics of nonlinear Coulomb friction, whose constant average value at unidirectional motion depends on the motion sign only, after the transient presliding phase at each motion reversal. In this work, we analyze and demonstrate the use of Prandtl-Ishlinskii operators for modeling the Coulomb friction with presliding phase. No viscous i.e. velocity-dependent component is considered at this stage, and the constant damping rate of the Coulomb friction is combined with the rate-independent losses of presliding hysteresis. The general case of Prandtl-Ishlinskii operator with a continuous distribution function is considered together with a finite elements case, which is useful for implementation in multiple applications. Finally, identification of parameters is addressed and discussed along with two experimental examples.

1. INTRODUCTION

Coulomb friction [1], which is well-established and often understood as a "classical" dry friction law, expands the Amontons' theory, which postulates that the tangential friction force F is μ-proportional to the normal load L. Coulomb postulated the dry friction law of the form

$$F = \mu L + C \,, \tag{1}$$

where the correction term C allowed for dependence of the friction force on the surface reactions on a microscopic (molecular) level, such as surface asperities in contact, and is independent of the normal loading and contact surface [2]. The standard notation of the Coulomb friction law for steady-state kinetic friction assumes a discontinuous dependence of the friction coefficient on the relative sliding velocity $\dot{y}$, so that

$$F = \mu L \operatorname{sign}(\dot{y}) \,. \tag{2}$$

For constant normal loads and homogenous, time-invariant, frictional surfaces, a lumped Coulomb friction coefficient $\mu L := F_c$ is usually assigned. In order to avoid discontinuity

in the Coulomb friction law (2), and therefore make it appropriate for numerical simulations and control applications, in particular at zero velocity crossing, several empirical and heuristic approaches have been proposed for capturing the so-called presliding behavior of kinetic friction (see e.g. [3, 4] for details). Examples of such approaches include the Dahl model [5], Maxwell-slip model [6], modified Maxwell-slip model [7]. Note that more comprehensive dynamic friction models, such as LuGre model [8], generic model at asperity level [9], and two-state dynamic friction model with elasto-plasticity [10], also incorporate the presliding friction behavior. The presliding friction effects have been observed in various tribological and other friction-related experiments, see e.g. [3, 11, 12, 13].

An interesting fact is that the so-called Maxwell-slip model structure [6] coincides with the Prandtl-Ishlinskii (PI) stop-type hysteresis model, for details on the latter we refer to [14, 15, 16]. This model relies on elementary Prandtl-Ishlinskii stop-type hysteresis operators, which are rheological elements well established for describing effects of elasto-plasticity. The Prandtl-Ishlinskii stop-type hysteresis operator is dual to the Prandtl-Ishlinskii play-type operator (see e.g. [16] for details) which, in turn, is well-known in mechanics and is used for describing the kinematic play, also known as backlash, in the machine elements and mechanisms. The Prandtl-

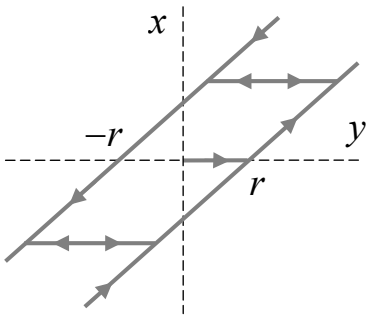

Figure 1. Prandtl-Ishlinskii play-type operator transitions.

Ishlinskii play-type operator is schematically illustrated in Figure 1. The operator provides a rate-independent map of time series y to time series x, which can be considered in various functional spaces such as $W^{1,1}$, C, BV and the space of regulated functions. This map depends on the initial state x_0 and threshold parameter $r > 0$. The latter determines the width $2r$ of the play-zone. The operator in the differential form is given by

$$\dot{x} = \begin{cases} \dot{y} & \text{if } \; x = y - r, \; \dot{y} \geq 0 \,, \\ \dot{y} & \text{if } \; x = y + r, \; \dot{y} \leq 0 \,, \\ 0 & \text{if } \; y - r < x < y + r \,, \end{cases} \qquad |x - y| \leq r \tag{3}$$

for a.e. $t \geq t_0$.

The general Prandtl-Ishlinskii model is formulated as a superposition (parallel connection) of elementary stop-type operators. A set of free parameters is used to map the distribution of elementary stop-type operators to the actual shape of hysteresis loops of the Prandtl-Ishlinskii model. Actually, it is the initial loading curve, often referred to as the "virgin curve" [17] (due to the memory-free "virgin" contacts on the frictional interface) that determines the shape of the force-displacement transitions and therefore the presliding friction hysteresis. According to Madelung's rules originally proposed in magnetism [18], and quite similar Masing's rules with origins in structural mechanics [19], measuring the initial loading curve is sufficient for a complete identification of parameters of the Prandtl-Ishlinskii hysteresis model.

The aim of this paper is to discuss how the Prandtl-Ishlinskii hysteresis operators can be efficiently used for modeling nonlinear Coulomb friction with presliding hysteresis transitions. In real-life mechanical systems to be simulated and controlled the problem of Coulomb friction discontinuity is one of the most crucial issues for proper system analysis, proof of stability, and control design. An appropriate incorporation of presliding phase into Coulomb friction law is an essential condition for the model-based analysis of system dynamics, damping properties, and synthesis of friction compensation methods. In particular, motion control problems of exact positioning type, see e.g. [20, 21], require a better perception of presliding friction behavior at the motion onset and reversals. Presliding friction effects are particularly important in such applications as rolling bearing nanopositioning stages [22], hard disk drives [23], ball-screw-driven positioning stages [24], hydraulic cylinders [25], and others.

Several strong assumptions are made here in relation to the friction behavior to be considered:

(i) No viscous (proportional to the relative velocity) friction effects are included.

(ii) The breakaway (static friction) force due to adhesion is not considered so that no velocity weakening [4], also referred to as Stribeck effect, occurs at the transients between the presliding and gross sliding regimes.

(iii) The so-called smooth sliding with the averaged constant Coulomb friction force is considered. Hence, true stick-slip dynamics on the atomic level of frictional interfaces with related Frenkel-Kontorowa and Prandtl-Tomlinson type interactions (see [26, 27] for details) are not addressed.

The paper is organized as follows. The finite elements case with a finite number of Prandtl-Ishlinskii (PI) stop-type operators and one additional discontinuous element required for the motion system to be asymptotically stable is described in Section 2. The general Prandtl-Ishlinskii operator with a continuous distribution function is discussed in Section 3. Estimation and identification of free parameters for the proposed modeling approach is discussed in Section 4, where we also present two experimental examples. Section 5 contains conclusions.

2. FINITE ELEMENTS CASE

In the finite elements case, a parallel connection of N single elasto-plastic elements with a common input is considered. Due to their superposition and the absence of coupling between the elements, the total output friction force is given by simple superposition

$$F(y) = \sum_{j=1}^{N} F_j \, . \tag{4}$$

Note that the input argument in (4), which is the same for each single elasto-plastic element, is the relative displacement y and not the relative velocity $\dot{y}$, as it is assumed in the general case of kinetic friction addressed in Section 1. However, a differential form of PI operators with $\dot{y}$ used as the input is also available, see e.g. in [28]. Recall that each elasto-plastic element j representing a stop-type PI operator can be described by

$$F_j = k_j f_j, \qquad f_j = y - x_j(y, r_j) \, , \tag{5}$$

where k_j is the stiffness coefficient, f_j is the elastic deformation, and x_j is the output state of the corresponding play-type operator illustrated in Figure 1. The free parameters are the individual break-away force level c_j and presliding stiffness k_j of each elementary elasto-plastic element. These two parameters are related through the threshold value of the play-type PI operator, i.e.

$$r_j = c_j / k_j \, . \tag{6}$$

One can recognize that both parameters control the individual transition between presliding and sliding and therefore determine piecewise linear segments of the force-displacement presliding hysteresis curve. An example of such curve with three elasto-plastic elements is schematically illustrated in Figure 2. The shadowed regions characterize the presliding range. It is important

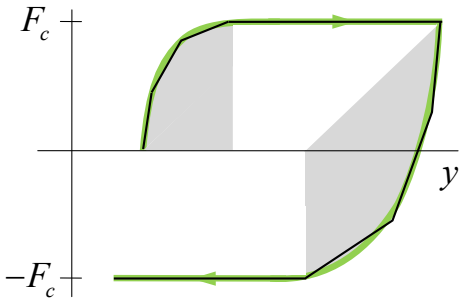

Figure 2. Presliding friction behavior and its piecewise linear approximation.

to note that after each motion reversal and at the onset of relative motion, each elasto-plastic element in the structure is first sticking before passing into the sliding. Therefore, the initial presliding stiffness after each motion reversal, which occurs at a relative position $y(t_r)$, is equal to the cumulative stiffness of all elasto-plastic elements so that

$$\frac{\partial F(t_r^+)}{\partial y(t_r^+)}\Big|_{y=y(t_r)} = \sum_{j=1}^{N} k_j \,. \tag{7}$$

It has been shown in [28] that for an unforced motion system (with friction force F) to be globally asymptotically stable in the Lyapunov sense, i.e. to have the global zero motion equilibrium, at least one elasto-plastic element should have $k_j \to \infty$ (see Corollary 2 in [28]). In other words, after each motion reversal at least one elasto-plastic element is immediately in sliding. This corresponds to a constant Coulomb-type friction force with discontinuity at the velocity zero-crossing. Recall that the overall Coulomb friction force with discontinuity, i.e. $F \sim \mathrm{sign}(\dot{y})$, constitutes the limit case of presliding hysteresis curves at motion reversals, see [29] for details.

In order to illustrate the initial stiffness behavior of presliding friction hysteresis, consider a finite elements case with $N = 3$ stop operators with $c_{1-3} = [1,\ 1,\ 1]$. We set $k_{2,3} = [10,\ 4]$, and vary the stiffness of the first element by an order of magnitude, $k_1 = \{500,\ 50,\ 5\}$. Friction-displacement hysteresis curves obtained from the same input sequence are shown in Figure 3.

In order to make the finite elements friction modeling globally asymptotically stable, equation (4) should be modified in such a way that at least one element does not exhibit an elastic phase and passes into sliding immediately after each motion reversal. This can be achieved by adding the Coulomb friction law with discontinuity, thus yielding

$$F(y, \dot{y}) = c_1 \,\mathrm{sign}(\dot{y}) + \sum_{j=2}^{N} F_j \,. \tag{8}$$

It is obvious that $0 < c_1 < F_c$ should hold while

$$\sum_{j=1}^{N} c_j = F_c \,, \tag{9}$$

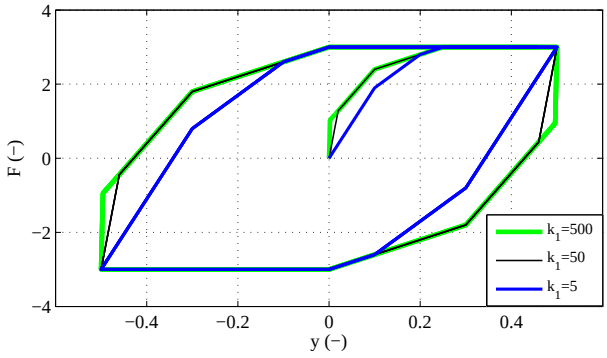

Figure 3. Presliding friction hysteresis curves for a varying stiffness of one elasto-plastic element within the model with 3 PI stop-type operators.

where F_c is the Coulomb friction coefficient, which determines the maximal friction amplitude at unidirectional motion. Several important properties of the presliding friction behavior can be derived for model (8):

- For $c_1 > 0$, the total friction behavior has infinite stiffness at each motion reversal, independent of presliding or sliding state in the relative force-displacement coordinates. This is in accord with stiction friction phenomenon, for which a certain amount of external force is first required to move an idle motion system with friction from zero equilibrium.
- If the elementary stiffnesses satisfy $k_j \to \infty$ for all $j \in [2, \ldots, N]$, then the total friction force satisfies $F(y, \dot{y}) \to F_c \operatorname{sign}(\dot{y})$, which corresponds to the "classical" Coulomb friction law and represents the limit case of presliding hysteresis friction.
- With $N \to \infty$, the friction force equation (8) can be transformed into the general PI model considered in the next section.

3. GENERAL CASE

A more general Maxwell-slip friction model includes an infinite number of stop-type PI operators parameterized by the threshold r, which ranges over an interval of values $0 \le r \le R$. Using this formalism, the friction force can be modeled by the following counterpart of relation (8):

$$F(y, \dot{y}) = c_1 \operatorname{sign}(\dot{y}) + \int_0^R f(y, r)\, d\mu(r) \tag{10}$$

with the normalized force $f(r)$ (or, equivalently, elastic deformation) given by

$$f(y, r) = y - x(y, r)\,, \tag{11}$$

where $x(y, r)$ is the output state of the play-type PI operator, which has threshold r (cf. Figure 1). The term $c_1 \operatorname{sign}(\dot{y})$ in (10) corresponds again to the element with infinite stiffness. The Riemann-Stieltjes integral with a distribution function μ in (10) is a PI operator of general type [14].

In particular, with a piecewise constant distribution

$$\mu(r) = \sum_j^N k_j H(r - r_j),$$

where H is the Heaviside step function, formula (10) with $R > \max r_j$ reduces to the finite elements case (8).

If the distribution function μ is continuous, then the unforced motion system with friction (10) is globally asymptotically stable even in the case when $c_1 = 0$, i.e. stiffness is uniformly bounded for all elements (see [28]). This is because for any motion, elements with a sufficiently small threshold r are always in sliding, hence any motion dissipates energy due to friction. This can be compared to the finite elements case (8), in which sufficiently small oscillations do not dissipate energy because all the elements are in pre-sliding mode, and the system effectively behaves as a harmonic oscillator. If $c_1 = 0$, then the motion system with a continuous distribution function μ will produce infinitely many damped oscillations of decreasing vanishing amplitude. On the other hand, if $c_1 > 0$ (i.e. there is an element with infinite stiffness), then the motion comes to a complete stop after a finite number of oscillations both in cases of discrete-valued and continuous μ distribution.

Assuming the lumped unity mass (i.e. $m = 1$), the equation of free motion with friction (10) has the form

$$\ddot{y}(t) + c_1 \operatorname{sign}\big(\dot{y}(t)\big) + \int_0^R f\big(y(t), r)\big)\, d\mu(r) = 0\,, \tag{12}$$

and the total energy of this system is

$$E = \frac{1}{2}\Big(\dot{y}^2 + \int_0^R \big(f(y, r)\big)^2\, d\mu(r)\Big)\,.$$

Note that the maximal elastic force associated with the integral term in (12) equals

$$F_m = \int_0^R r\, d\mu(r).$$

Clearly, if the stiction friction level exceeds this force,

$$c_1 > F_m,$$

then any free motion of the mass m will proceed in the direction of the initial momentum until, after a finite time, the mass will come to a complete stop because the static friction will balance the elastic force at the stopping point.

Now, assuming that the opposite inequality holds, $c_1 < F_m$, and the initial momentum (energy) is sufficiently large, let us consider the conditions, which ensure that the trajectory makes one turning point before the motion comes to a complete stop. Without loss of generality, let us suppose that the initial momentum is negative and place the origin, $y = 0$, at the first turning point of the motion. Then, the second turning point satisfies $y_e > 0$. If the initial momentum is sufficiently large, then the elastic force at the first turning point is at its maximal value F_m, and the equation of motion between the first turning moment t_1 when $y(t_1) = 0$ and the second turning moment t_2 when $y(t_2) = y_e$ reads

$$\ddot{y}(t) + c_1 + \Phi\big(y(t)\big) = 0 \tag{13}$$

with the elastic force given by

$$\Phi(y) = \int_0^{y/2} r\, d\mu(r) + \int_{y/2}^R (y - r) d\mu(r)\,, \tag{14}$$

where y increases from $y(t_1) = 0$ to $y(t_2) = y_e$ and $\dot{y}(t_1) = \dot{y}(t_2) = 0$. Multiplying (13) by $\dot{y}$ and integrating the resulting equation from t_1 to t_2 yields the following equation for the second turning point y_e:

$$c_1 y_e + \int_0^{y_e} \Phi(y)\, dy = 0\,. \tag{15}$$

The motion comes to a complete stop at this point if the stiction friction level exceeds the elastic force, that is if

$$c_1 > \Phi(y_e). \tag{16}$$

Thus, the free motion with a sufficiently high initial momentum exhibits exactly one reversal (turning point) before coming to a complete stop if condition (16) holds for the smallest positive root y_e of equation (15) with the function Φ defined by (14). Continuing the same line of argument, one obtains similar conditions, which ensure that the motion stops after making exactly n reversals.

4. IDENTIFICATION OF PARAMETERS

In most cases, the identification of parameters of the friction model is done on a real motion system, for which both a moving mass (inertia) and frictional contact interface constitute the given physical matters. Assuming a general driving input force u, which can be the control value, and the lumped mass m, the motion dynamics with friction (8) is described by

$$m\ddot{y}(t) + c_1 \operatorname{sign}\big(\dot{y}(t)\big) + \sum_{j=2}^{N} k_j\big(y(t) - x_j(y, r_j)\big) = u(t) \tag{17}$$

(cf. (12)). Assuming that the control value $u(t)$, relative displacement $y(t)$ and at least its first time derivative are the measurable quantities, the model identification reduces to finding of the best-fit of the free parameters (friction model and mass) based on the generated and recorded experimental data. Here the model identification errors can be built based on either motion or force quantities, i.e. forward or inverse model, while the other signals constitute the available regressors for identification. All the residual parameters, with the exception of thresholds of stop-type operators, contribute linearly to (17), makes the identification procedure straightforward. According to [30] and [31], both linear regression (LS) and nonlinear regression (NLS) approaches are well suited for indentifying the Maxwell-slip-type structure, which is equivalent to the PI model. For the LS approach, a pre-assignment of elements' threshold values (equivalent to the break-away force level) is however required, since these are not linear parameters according to from (17). Various numerical routines are available for solving either LS or NLS problem related to (17). Here we abstain from presenting details of identification algorithms and instead refer to the fundamental literature on system identification, e.g. [32].

Two experimental tests, both aimed at comparing the measured and modeled motion response in vicinity of an equilibrium state, i.e. full motion stop, are presented below. We note that before the full stop the moving mass can exhibit at least one detectable reversal. This effect is due to a finite non-zero inertia, which is antagonized by presliding friction with elasto-plastic interactions on the contact interface. The targeted motion phase represents an unforced system dynamics (equation (17) with zero right-hand-side) with non-zero initial conditions which are detectable from the available measurements. This operation regime is particularly suitable for exposing the presliding friction and contact stiffness at motion reversals.

In both experimental tests shown below, the identified parameters of the model with four elasto-plastic elements ($N = 5$) are m, F_c, c_1, k_2, k_3, k_4, and k_5. For the sake of simplicity and in order to avoid local minima during the curves fit, the break-away force level of the single stop-type elements are assumed to have one and the same value $c_{2-5} = (F_c - c_1)/4$. This is a

reasonable pre-assignment for mapping the initial loading curve when the number of elements equals to or exceeds 3 (for more details see the identification results in [31, 33]).

Experimental test I
The first experimental test, the same as reported in [28, 29], represents a steady-state motion with the constant velocity at constant (control) input force at the beginning. Afterwards, the control input is switched-off and the relative motion decelerates to zero being driven by the counteracting friction only. The control signal and the measured relative velocity are shown in Figure 4. An almost linear slope of the decreasing relative velocity points to the predominance of the constant Coulomb friction force for which the unforced motion dynamics is $\ddot{y} = -(F_c/m)\,\mathrm{sign}(\dot{y})$. After the first velocity zero-crossing, a low negative overshoot occurs, which is the motion reversal followed by a low-velocity displacement (at time between 0.09 sec and 1.13 sec) before the final motion stop. Note that the depicted relative velocity is the discrete-time derivative of the recorded incremental encoder signal. Therefore the pulsed pattern does not imply any measurement noise but the actual low velocity, which is inherently subject to the discretization and quantization effects. The same can be said about the measured velocity pattern during the decreasing slope related to the constant deceleration. The identified model

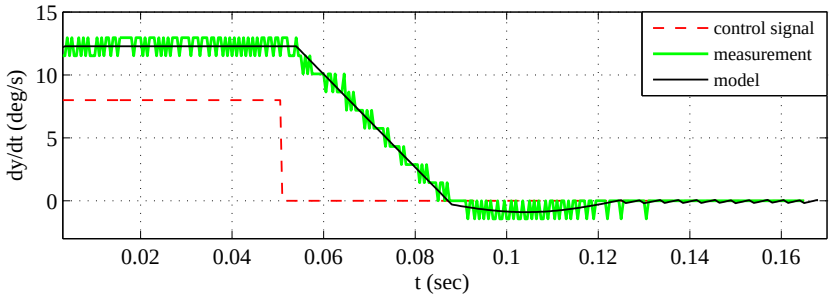

Figure 4. Experimental test I (measurement and model): velocity response in a vicinity of the motion stop after switching off the constant control force.

response is shown in Figure 4 over the measurement. The curve's best-fit exhibits, however, some residual micro-oscillations related to the numerical computation of (17), since the sign-discontinuity is incorporated.

Experimental test II
In the second experimental test, the measured data are taken from the free (unforced) system, which has been first excited by an input impulse. The data that we use is close to the motion stop and discards the transients, which can include the non-modeled high-frequency components coming from the unaccounted flexibilities in the system. The measured velocity response under consideration is depicted in Figure 5(a). Note that the experimental motion system is without gearing mechanisms, in contrast to Experimental test I, and is equipped with an angular encoder of higher resolution. This becomes apparent when comparing the increments of the measured velocity patterns in Figures 4 and 5(a). The negative velocity pattern after the first zero-crossing is more accurately captured. This provides a more detailed signature of presliding friction after the motion reversal. The details about experimental setup, from which the measured data has been obtained, can be found in [34]. The fitted model response shown in Figure 5(a) demonstrates an accurate match with the measured data. The accuracy of the fitted model becomes further apparent when analyzing the corresponding phase portrait depicted in Figure 5(b). Here the model-based prediction of relative displacement carries weight in order to decrease

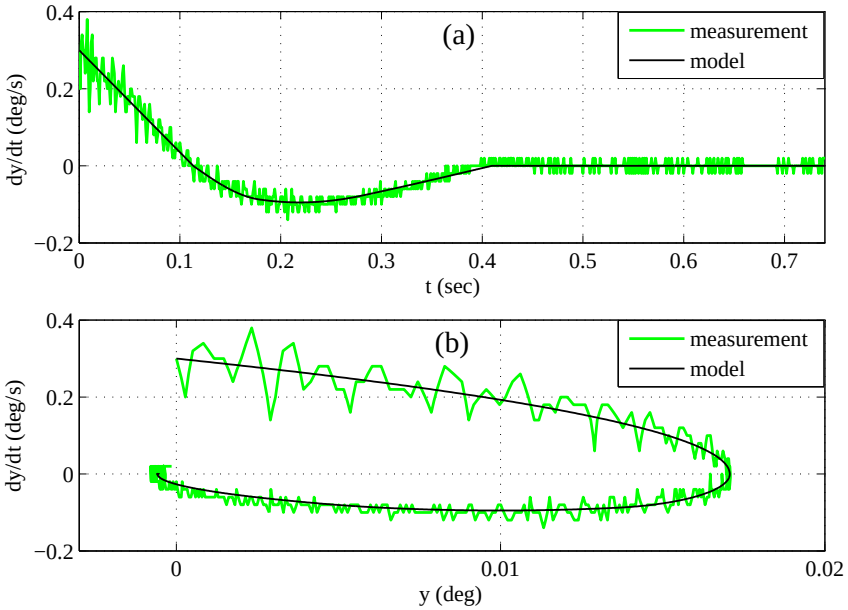

Figure 5. Experimental test II (measurement and model): (a) velocity response in vicinity the motion stop; (b) displacement-velocity phase portrait.

an integral error. From both the measured and modeled phase portraits, a marginally visible second motion reversal can be also recognized. However, this apparently lies beyond the available measurement accuracies and is not analyzed here.

5. CONCLUSIONS

In this paper, we have explored how the Prandtl-Ishlinskii stop-type hysteresis model, which is equivalent to the Maxwell-slip structure, can be used for describing the kinetic Coulomb friction including the presliding phase. The latter is characterized by the rate-independent force. The so-called initial loading ("virgin") curves determine the shape of hysteresis loops and damping characteristics of the unforced motion before the final motion stop. Finite elements and general continuous distributions have been addressed, and the parameters identification has been demonstrated with two experimental examples. We have identified conditions which ensure that the motion stops after a given number of reversals. It would be interesting to consider a counterpart of equation (17) with interacting stop nonlinearities, for example using the techniques developed in [35, 36, 37, 38].

Acknowledgments

D. Rachinskii acknowledges the support of NSF through grant DMS-1413223.

References

[1] de Coulomb C A 1785 *Memoire de Mathematique et de Physics de l'academie Royal* 161–342
[2] Awrejcewicz J and Olejnik P 2005 *Applied Mechanics Reviews* **58** 389–411
[3] Armstrong B, Dupont P and De Wit C C 1994 *Automatica* **30** 1083–1138
[4] Al-Bender F and Swevers J 2008 *IEEE Control Systems Magazine* **28** 64
[5] Dahl P R 1968 A solid friction model TOR 158(3107-18) The Aerospace Corporation, El Segundo
[6] Lazan B J 1968 *Damping of materials and members in structural mechanics* vol 214 (Pergamon press Oxford)
[7] Ruderman M and Bertram T 2011 *IFAC Proceedings Volumes* **44** 10764–10769 18th IFAC World Congress
[8] De Wit C C, Olsson H, Aström K J and Lischinsky P 1995 *IEEE Trans. on automatic control* **40** 419–425

[9] Al-Bender F, Lampaert V and Swevers J 2004 *Tribology Letters* **16** 81–93
[10] Ruderman M and Bertram T 2013 *Mechanical Systems and Signal Processing* **39** 316–332
[11] Koizumi T and Shibazaki H 1984 *Wear* **93** 281–290
[12] Bowden F P and Tabor D 2001 *The friction and lubrication of solids* vol 1 (Oxford university press)
[13] Lampaert V, Al-Bender F and Swevers J 2004 *Tribology Letters* **16** 95–105
[14] Krasnosel'skii M and Pokrovskii A 1989 *Systems with Hysteresis* (Springer)
[15] Visintin A 1994 *Differential models of hysteresis* (Springer)
[16] Krejci P 1996 *Hysteresis, Convexity and Dissipation in Hyperbolic Equations* (Tokyo: Gattötoscho)
[17] Al-Bender F, Symens W, Swevers J and Van Brussel H 2004 *International journal of non-linear mechanics* **39** 1721–1735
[18] Madelung E 1905 *Annalen der Physik* **322** 861–890
[19] Masing G and Mauksch W 1925 *Wissenschaftliche Veröffentlichungen aus dem Siemens-Konzern* 244–256
[20] Ruderman M and Iwasaki M 2016 *IEEJ Journal of Industry Applications* **5** 61–68
[21] Ruderman M 2016 *IFAC-PapersOnLine* **49** 82–86
[22] Dong X, Yoon D and Okwudire C E 2017 *Precision Engineering* **47** 375–388
[23] Yan T and Lin R 2003 *IEEE Transactions on Magnetics* **39** 1064–1069
[24] Zhu H and Fujimoto H 2015 *IEEE/ASME transactions on mechatronics* **20** 956–966
[25] Tran X B, Hafizah N and Yanada H 2012 *Mechatronics* **22** 65–75
[26] Urbakh M, Klafter J, Gourdon D and Israelachvili J 2004 *Nature* **430** 525–528
[27] Popov V and Gray J 2012 *ZAMM - J. of Applied Math. and Mech.* **92** 683–708
[28] Ruderman M 2015 *Mechatronics* **30** 225–230
[29] Ruderman M and Iwasaki M 2016 *Journal of Physics: Conf. Series* **727** 012014
[30] Al-Bender F, Lampaert V and Swevers J 2004 *Chaos* **14** 446
[31] Rizos D and Fassois S 2009 *IEEE Transactions on Control Systems Technology* **17** 153–160
[32] Ljung L 1999 *System Identification: Theory for the User* 2nd ed (Prentice Hall)
[33] Al-Bender F, Lampaert V, Fassois S, Rizos D, Worden K, Engster D, Hornstein A and Parlitz U 2003 *Nonlinear Dynamics of Production Systems* 349–367
[34] Ruderman M, Aranovskii S, Bobtsov A and Bertram T 2012 *Automation and Remote Control* **73** 1604–1615
[35] Krejci P, Lamba H, Melnik S and Rachinskii D 2014 *Phys. Rev. E* **90** 032822
[36] Krejci P, Lamba H, Melnik S and Rachinskii D 2015 *Discrete and Continuous Dynamical Systems B* **20** 2949–2965
[37] Krejci P, O'Kane P, Pokrovskii A and Rachinskii D 2012 *Physica D* **241** 2010–2028
[38] Krejci P, Lamba H, Antunes G and Rachinskii D 2016 *Mathematica Bohemica* **141** 261–286